# GEOLOGICAL SURVEY OF CANADA
# OPEN FILE 7856

# Targeted Geoscience Initiative 4: Canadian Nickel-Copper-Platinum Group Elements-Chromium Ore Systems — Fertility, Pathfinders, New and Revised Models

## Trace element distribution in sulphide assemblages of the Levack-Morrison ore system, Sudbury, Ontario: Looking for chemical fingerprints of mineralization processes

**Moji Adibpour[1], Pedro J. Jugo[1], and Doreen E. Ames[2]**

[1]Laurentian University, Sudbury, Ontario
[2]Geological Survey of Canada, Ottawa, Ontario

# 2015

This publication is available for free download through GEOSCAN (http://geoscan.nrcan.gc.ca/)

Publications in this series have not been edited; they are released as submitted by the author.

**Contribution to the Geological Survey of Canada's Targeted Geoscience Initiative 4 (TGI-4) Program (2010–2015)**

# TABLE OF CONTENTS

# Trace element distribution in sulphide assemblages of the Levack-Morrison ore system, Sudbury, Ontario: Looking for chemical fingerprints of mineralization processes

Moji Adibpour[1]*, Pedro J. Jugo[1], and Doreen E. Ames[2]

[1]Department of Earth Sciences, Laurentian University, 935 Ramsey Lake Road, Sudbury, Ontario P3E 2C6
[2]Geological Survey of Canada, 601 Booth Street, Ottawa, Ontario K1A 0E8
*Corresponding author's e-mail: mx_adibpour@laurentian.com

## ABSTRACT

One challenge in the exploration for Cu-Ni-PGE mineralization in the footwall of the Sudbury Igneous Complex (SIC) is the uncertainty of its origin. The relative proximity of mineralization to the SIC is consistent with models of magmatic fractionation, but the common association of ore in the SIC footwall with amphibole and epidote alteration is consistent with a hydrothermal origin. Although these processes are not mutually exclusive (e.g. ores of magmatic origin could have been later remobilized by hydrothermal fluids), better constraints on which processes operated would greatly assist exploration. This project is a pilot study to assess whether chemical fingerprints can be established for four distinct mineralization types in the Levack-Morrison ore system: (a) contact; (b) a transition zone between contact and footwall ore; (c) sharp-walled veins; and (d) disseminated, S-poor, PGE-rich ores.

Sulphide assemblages consisting primarily of pyrrhotite, chalcopyrite, and pentlandite were characterized in detail (petrography, SEM, EPMA, LA-ICP-MS). The results indicate that (a) Se content increases with depth; and (b) some trace elements (e.g. Cd vs. Se in chalcopyrite, Co vs. Se in pentlandite and pyrrhotite) can discriminate among different ore types. Calculated partition coefficients ($\pm 2\sigma$) for Se in chalcopyrite and pentlandite ($1.2 \pm 0.1$ for contact and transition ores, $0.5 \pm 0.2$ for sharp-walled veins) are significantly different, which is consistent with different mineralization processes for those ore types. In addition to trace element content calculation in major sulphides, element distribution maps were created from LA-ICP-MS spectra of sulphide assemblages. Some contact-style samples contained abundant euhedral pyrite but pyrite was also present in samples of other ore types. The maps showed complex trace element zonation (e.g. Se, Co, and As) in pyrite in contact ore, as well as some PGE minerals (notably Ir and Os). In contrast, no PGEs were detected in any of the other sulphides or any compositional zoning. Because Ir has very low solubility under most hydrothermal conditions, Co-rich, Ir-bearing pyrite was interpreted to have formed from the cooling of a sulphur-rich sulphide liquid. Such pyrite (when present) could be used as an indicator of a magmatic signature.

To further refine these results, future work would need to focus on three areas: (1) analyses of additional samples from the Morrison-Levack ore system to validate the discrimination diagrams for different ore types; (2) similar work would need to be undertaken elsewhere in the Sudbury mining district, to establish if the proposed discrimination plots are applicable basin-wide; (3) better constraints would need to be established for the origin of the Co-rich, PGE-bearing pyrite to enable it to be used as a marker of ore type.

## INTRODUCTION

The 1.85 Ga Sudbury impact structure, located at the boundary between the Archean Superior Province and the Proterozoic Huronian Supergroup of the Southern Province (Fig. 1a), hosts some of the largest Ni-Cu-platinum group element (PGE) resources in the world (Ames and Farrow, 2007). The Ni-Cu-PGE ore deposits in the Sudbury District have been divided into three main types: (1) contact-type deposits, with sulphides concentrated in embayments near the base of the Sudbury Impact Complex (SIC); (2) offset-type deposits, hosted by radial and concentric offset dykes; and (3) footwall-type deposits, hosted by shock-derived impact breccia in the SIC footwall (Morrison et al., 1994). Figure 1b shows the schematic relationship between contact-type mineralization and footwall ores. The magmatic origin of high-Ni, low-PGE contact-type deposits has been reasonably well established.

**Figure. 1.** Sample location. a) Location of Levack-Morrison deposit on the north Range of the Sudbury Igneous Complex (modified from Ames and Farrow, 2007). **b)** Schematic section of the contact, transition, and footwall orebodies that define the Levack-Morrison ore system (after Ames and Farrow, 2007). **c)** Three-dimensional projection of the contact Levack deposit (purple) and footwall Morrison deposit (red) orebodies showing the locations of samples (green) used in this study (after Ames and Kjarsgaard, 2013).
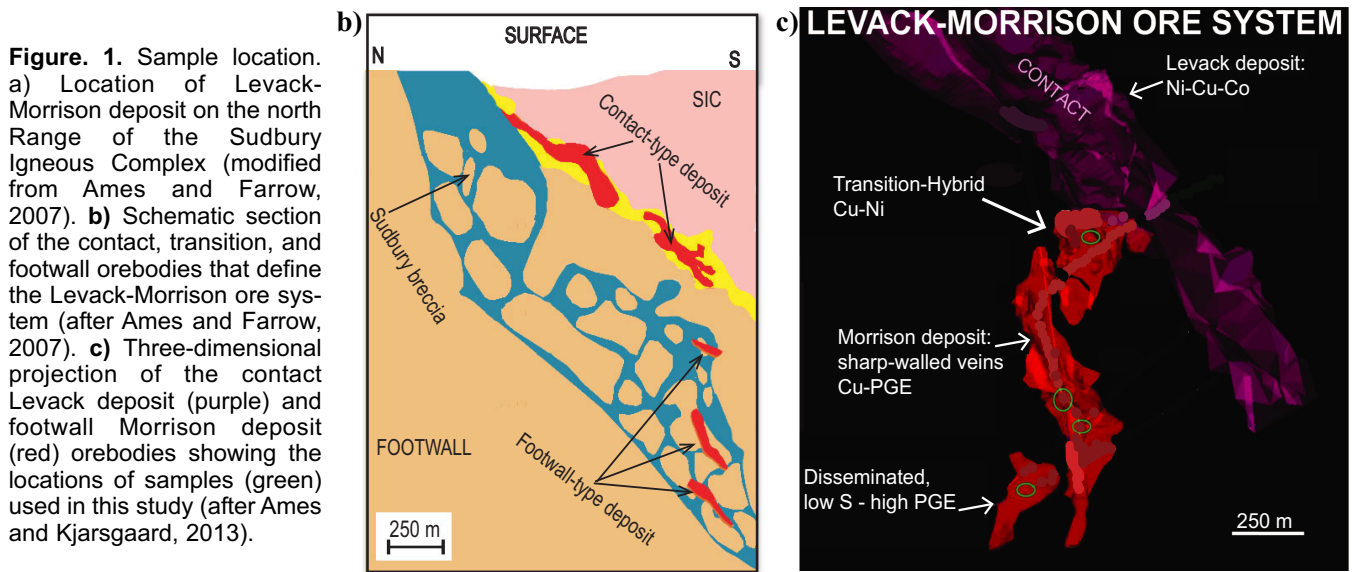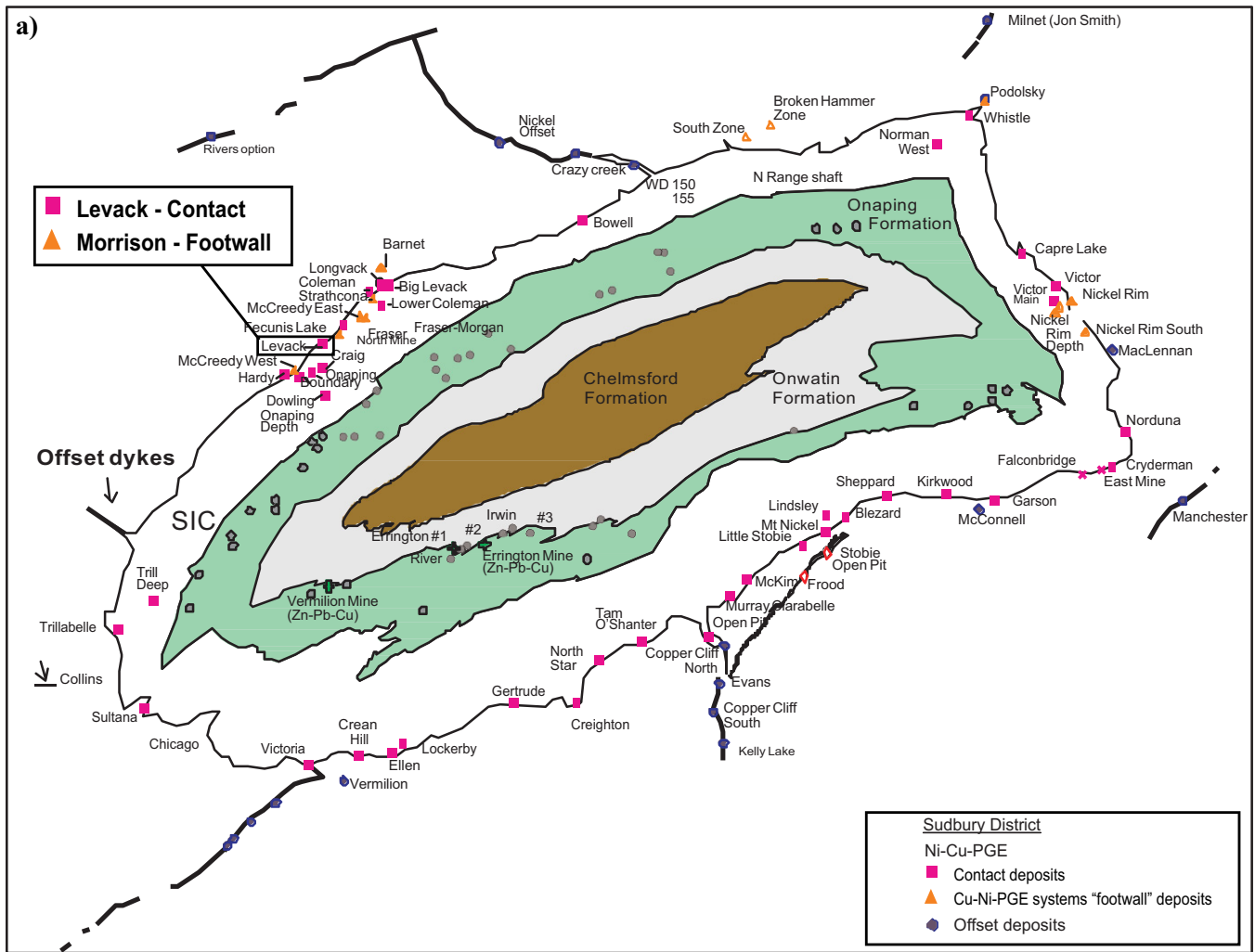
These deposits are widely recognized as segregations of immiscible sulphide melts that accumulated along the floor and embayments of the SIC during cooling of the impact melt sheet after meteoritic impact (Ames and Farrow, 2007). In contrast, the origin of mineral-ization within the footwall is not well understood, in part because of the different styles of mineralization that are present. Kjarsgaard and Ames (2010) showed that mineral assemblages in the footwall ores have been affected by multiple processes (magmatic, meta-

morphic, and hydrothermal). It has been hypothesized that the footwall ore deposition was related to magmatic processes (e.g. Stewart and Lightfoot, 2010); in contrast, the quartz, epidote, and amphibole alteration assemblages may indicate mineralization by hydrothermal or metamorphic processes (e.g. Farrow and Watkinson, 1997; Gibson, 2010). In order to develop a good exploration model for mineralization related to the footwall of the SIC, it must be established to what extent the mineralization was directly related to sulphide melts (i.e. directly related to the impact event) and or related to deposition from subsequent hydrothermal fluids.

The Levack-Morrison ore system (Fig. 1c), on the north range of the SIC, is one of a few places in which a contact-type orebody (Levack) is in spatial continuity with the footwall ores (Morrison deposit). Mineralization within the Morrison footwall Cu-PGE-Ni ores can be divided in three mineralization types: (a) transition ore (with Ni ≈ Cu), which is a hybrid between contact and footwall-style mineralization; (b) sharp-walled veins (with Cu > Ni, PGE); and (c) low-S, high-PGE disseminated ore (Ames and Kjarsgaard, 2013). In general, transition, sharp-walled veins, and disseminated ores occur progressively deeper and away from contact-style ores. The primary goal of this project was to assess whether the trace element content in major sulphides (pyrrhotite, pentlandite, chalcopyrite) can be used to 'fingerprint' mineralization styles, and if so, which chemical fingerprints can be used as indicators for the different ore formation processes. In addition, element distribution maps were created to characterize and understand occurrences of Co-rich and PGE-bearing pyrite in contact-style deposits, and to test whether this type of pyrite is useful as an indicator of a specific mineralization process.

## RESULTS AND DATA ANALYSIS

### Samples and Methods

Fourteen samples from different sections of the Levack-Morrison ore system were analysed: three contact- type ore (Levack deposit); two from transition-type ore; two sharp-walled veins; three disseminated, low-sulphur, high-PGE ore. Sulphide assemblages were characterized under reflected light microscopy and SEM. Major element composition was obtained by electron probe microanalysis. Selected areas were analysed by LA-ICP-MS in two ways: (a) trace element content were obtained using spot analyses with a 90 μm laser beam diameter; (b) trace element distribution maps were created using a smaller laser beam diameter (~20 μm) for better spatial resolution. Trace element contents were obtained using Po725 a synthetic pyrrhotite standard and NIST-610 glass as cali-

bration standards. The Fe content of each mineral was used for internal standardization.

## Sulphide Mineralogy and Textures

Representative images of the samples analysed are shown in Figure 2. Samples from Levack (Fig. 2a) contain pyrrhotite, chalcopyrite, pentlandite, pyrite, and magnetite. Two types of pentlandite (blocky and flame) are present (Fig. 2b) as well as minor amounts of sphalerite and galena. Transition-type ore (Fig. 2c) contains massive pyrrhotite, chalcopyrite, blocky and flame pentlandite, and magnetite. Samples from sharp-walled veins (Fig. 2d) contain massive chalcopyrite-cubanite intergrowths, blocky and flame pentlandite, magnetite, and small amounts of sphalerite disseminated in chalcopyrite. Samples from low-sulphide, high-PGE disseminated ores (Fig. 2e) contain little sulphide, mostly as chalcopyrite, minor amounts of pentlandite, magnetite grains with ilmenite exsolution, very small (<50 μm) euhedral pyrite, and tiny (<50 μm) galena inclusions disseminated in chalcopyrite.

## Sulphide Composition

The composition of the sulphides is summarized in Table 1 (S, Fe, Cu, Ni, Co, Zn) and Table 2 (trace elements). Three different groups of elements were analysed: (a) highly siderophile elements (HSE = PGE plus Re and Au); (b) metalloids (As, Se, Sb, Te, Bi); (c) other chalcophile or siderophile elements (Co, Zn, Mo, Ag, Cd, Sn, Pb). Elements that were below detection limits (e.g. HSE) are not included in the Tables. Element distribution maps of sulphide assemblages are discussed below.

## DISCUSSION

### Chemical Fingerprinting and Geochemical Discrimination of Ore Types

One goal of this study was to identify elements that can be measured routinely, thus the focus was on elements that were consistently above detection limits. Elements that were too close to detection limits were deemed not reliable or useful because analytical uncertainties are deemed too high. Initially, Zn was targeted because Nelles (2012) noted a correlation between PGE and Zn content based on whole rock analyses, and Zn and Cd are markedly enriched in footwall Cu-PGE ores (Ames and Farrow, 2007). The working hypothesis was that because Zn partitions preferentially into Cu-rich melt, therefore the Zn content in chalcopyrite should track the fractionation of such melts. However, the Zn content in chalcopyrite was approximately the same for all the samples analysed. Revised petrography and SEM analyses revealed that all the samples contained sphalerite (often only as very small grains <50 μm), indicating that the Zn content in chalcopyrite is at spha-
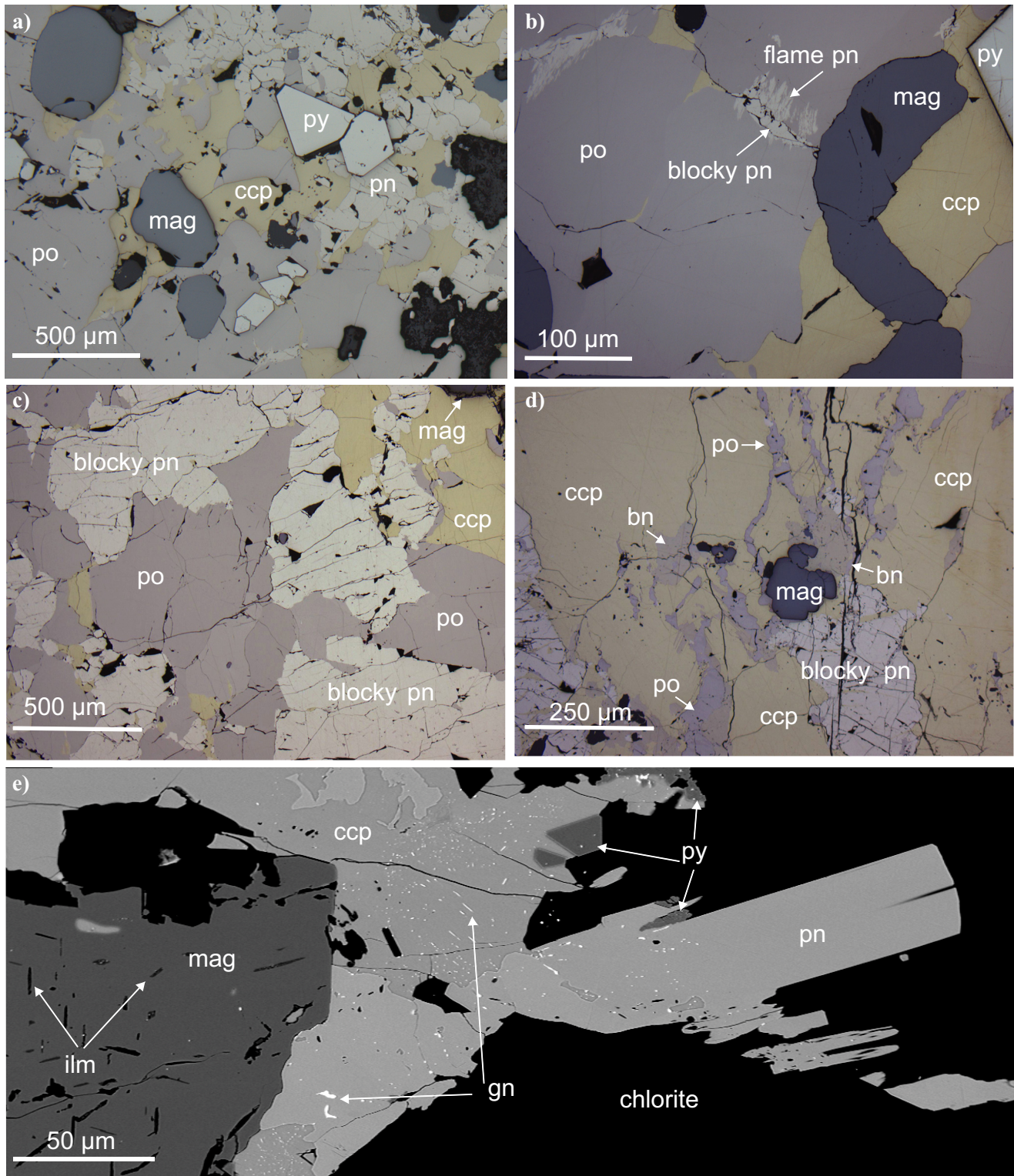
**Figure 2.** Ore textures and mineral associations in various ore types from the Levack-Morrison ore system. Typical assemblages contain variable amounts of chalcopyrite (ccp), magnetite (mag), pyrrhotite (po), and pentlandite (pn). **a)** Contact ore with euhedral pyrite (py) grains (sample 99AV-122). **b)** Detailed view of the two types of pn found in contact ore samples (sample 99AV-122). **c)** Footwall-contact transitional assemblage (sample 08AV-08) containing massive po, ccp, blocky and flame pn (similar to contact ore), and mag. **d)** Footwall sharp-walled veins (sample 05AV-11A) containing massive ccp in association with blocky and flame pn and strongly fractured anhedral to subhedral grains of mag. Pyrrhotite and bornite (bn) are minor phases in this sample. **e)** Backscattered electron image (BEI) of footwall-disseminated ore (sample 08AV-02A) showing ccp and minor amounts of pn and mag with ilmenite (ilm) exsolution, small galena (gn) inclusions disseminated in ccp, as well as small subhedral to euhedral py grains.

**Table 1.** Major element content (wt.%) of chalcopyrite, pentlandite, and pyrrhotite (by electron microprobe analysis) for the four types of mineralization present in the Levack-Morrison ore system in Sudbury Igneous Complex.

| Sample | n | | S | Fe | Cu | Ni | Co | Total |
|---|---|---|---|---|---|---|---|---|
| ***Chalcopyrite*** | | | | | | | | |
| 99AV-122 (Levack) | 7 | Ave. | 35.0 | 30.6 | 34.5 | <0.25 | | 100.1 |
| Contact | | Std. | 0.1 | 0.1 | 0.2 | | | |
| 08AV-08 (Morrison) | 8 | Ave. | 35.0 | 30.3 | 34.4 | <0.25 | | 99.6 |
| Transition | | Std. | 0.1 | 0.1 | 0.1 | | | |
| 05AV-11A (Morrison) | 8 | Ave. | 35.0 | 30.8 | 34.2 | <0.25 | | 100.0 |
| Sharp-walled veins | | Std. | 0.1 | 0.1 | 0.1 | | | |
| 08AV-02A (Morrison) | 1 | | 34.7 | 30.0 | 34.0 | <0.25 | | 98.6 |
| Disseminated | | | | | | | | |
| ***Pentlandite*** | | | | | | | | |
| 99AV-122 (Levack) | 15 | Ave. | 33.5 | 30.4 | <0.25 | 34.9 | 1.00 | 99.8 |
| Contact | | Std. | 0.2 | 0.6 | | 0.6 | 0.12 | |
| 08AV-08 (Morrison) | 11 | Ave. | 33.4 | 30.5 | <0.25 | 35.4 | 0.27 | 99.5 |
| Transition | | Std. | 0.1 | 0.2 | | 0.2 | 0.03 | |
| 05AV-11A (Morrison) | 8 | Ave. | 33.5 | 34.9 | <0.25 | 31.4 | 0.21 | 100.0 |
| Sharp-walled veins | | Std. | 0.2 | 0.1 | | 0.1 | 0.01 | |
| ***Pyrrhotite*** | | | | | | | | |
| 99AV-122 (Levack) | 10 | Ave. | 39.8 | 60.1 | <0.25 | 0.489 | 0.025 | 100.4 |
| Contact | | Std. | 0.1 | 0.1 | | 0.053 | 0.003 | |
| 08AV-08 (Morrison) | 8 | Ave. | 39.8 | 59.9 | <0.25 | 0.444 | 0.026 | 100.1 |
| Transition | | Std. | 0.1 | 0.2 | | 0.114 | | |
| 05AV-11A (Morrison) | 8 | Ave. | 39.1 | 61.5 | <0.25 | 0.072 | | 100.2 |
| Sharp-walled veins | | Std. | 0.1 | 0.1 | | 0.005 | | |

Note: n = sample size

lerite saturation, which renders Zn not useful for chemical fingerprinting in this system. Of the other elements that might be used to discriminate among the different ore types Se was the most notable. Selenium was chosen as the main variable for discrimination because it is present in all major sulphides and was shown to increase systematically with depth. For example, when Cd content in chalcopyrite is plotted versus Se content in chalcopyrite (Fig. 3a) there is a notable increase in Se content with distance from the contact ores; the Cd content helps separate the fields further although Cd content does not seem to systematically correlate with Se. Data from unaltered and slightly altered contact-style orebodies in McCreedy East (Dare et al., 2011) are shown for comparison (Fig 3a). The altered sample has higher Se and lower Cd, indicating that hydrothermal processes maybe responsible for the Se increase (and Cd decrease) relative to contact ores. However, the high Cd content in chalcopyrite from sharp-walled veins is not consistent with a hydrothermal origin. The As versus Se content in pentlandite (Fig. 3b) illustrates a similar behaviour to that Cd versus Se in chalcopyrite (Fig 3a), however, the Se content in pentlandite from sharp-walled veins (green triangles: Fig. 3b) is variable and has a positive correlation with As, indicating that both Se and As are compositionally zoned in pentlandite. Cobalt content in pentlandite (Fig. 3c) and in pyrrhotite (Fig. 3d) is significantly higher in contact ore than in other ore types, which also is an indicator that different ore processes involved in the formation of the contact ores relative to the footwall ores.

**Table 2.** Trace element content (in ppm) of chalcopyrite, pentlandite, and pyrrhotite (by electron microprobe analysis) for the four types of mineralization present in the Levack-Morrison ore system in Sudbury Igneous Complex.

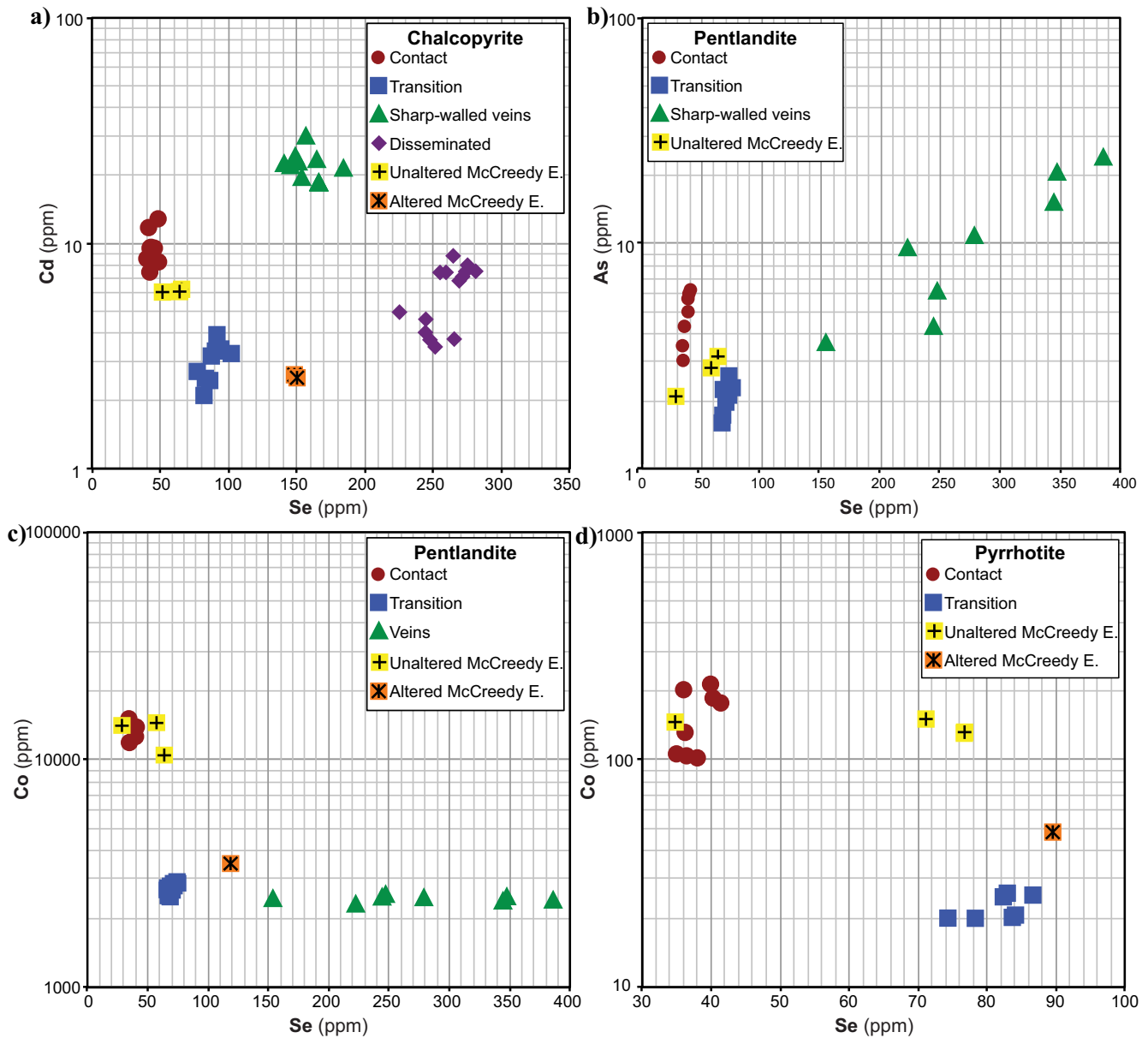| Sample | n | | Ag[109] | As[75] | Bi[209] | Cd[111] | Co[59] | Mo[95] | Pb[208] | Sb[121] | Se[77] | Sn[118] | Te[125] | Zn[66] | Zn[68] |
|---|---|---|---|---|---|---|---|---|---|---|---|---|---|---|---|
| ***Chalcopyrite*** | | | | | | | | | | | | | | | |
| Contact | 10 | Ave | 19 | 3.28 | 2.19 | 9.6 | 2.0 | 0.116 | 12.3 | 0.064 | 43.3 | 24.4 | 1.0 | 640 | 560 |
| (Levack; 99AV-122) | | Std | 17 | 0.36 | 0.95 | 2.0 | 1.8 | 0.065 | 4.7 | 0.028 | 1.7 | 3.6 | 1.6 | 150 | 120 |
| Transition | 9 | Ave | 2.9 | 3.3 | 0.046 | 3.00 | 1.3 | 1.9 | 14.7 | 0.059 | 88.3 | 2.53 | 0.090 | 488 | 440 |
| (Morrison; 08AV-08) | | Std | 1.0 | 1.4 | 0.026 | 0.53 | 1.6 | 1.6 | 6.4 | 0.016 | 6.7 | 0.72 | 0.061 | 55 | 55 |
| Sharp-walled veins | 8 | Ave | 11.0 | 2.12 | 0.058 | 23.5 | 0.095 | 0.059 | 46 | 0.050 | 155 | 81.5 | 5.9 | 560 | 467 |
| (Morrison; 05AV-11A) | | Std | 1.1 | 0.19 | 0.030 | 2.9 | 0.048 | 0.084 | 27 | 0.016 | 13 | 6.6 | 1.3 | 180 | 78 |
| Disseminated | 13 | Ave | 174 | 2.04 | 1.23 | 6.4 | 0.93 | 0.056 | 44 | 0.082 | 264 | 41 | 0.77 | 510 | 460 |
| (Morrison; 08AV-02A) | | Std | 34 | 0.16 | 0.66 | 1.8 | 0.91 | 0.021 | 32 | 0.016 | 11 | 13 | 0.18 | 170 | 150 |
| ***Pentlandite*** | | | | | | | | | | | | | | | |
| Contact | 7 | Ave | 2.29 | 4.8 | 4.3 | 0.50 | 13600 | 0.27 | 28 | 0.143 | 37.4 | 5.3 | 0.92 | 118 | 111 |
| (Levack; 99AV-122) | | Std | 0.76 | 1.1 | 2.2 | 0.29 | 1100 | 0.11 | 14 | 0.023 | 2.6 | 2.3 | 0.35 | 99 | 88 |
| Transition | 7 | Ave | 4.6 | 2.08 | 0.088 | 0.040 | 2750 | 0.79 | 5.4 | 0.046 | 70.0 | 0.065 | bdl | 2.4 | bdl |
| (Morrison; 08AV-08) | | Std | 1.0 | 0.30 | 0.041 | 0.026 | 110 | 0.80 | 2.4 | 0.016 | 2.1 | 0.043 | | 1.5 | |
| Sharp-walled veins | 9 | Ave | 39 | 13.3 | 0.58 | 0.51 | 2455 | 0.036 | 60 | 0.113 | 296 | 4.6 | 205 | 15 | bdl |
| (Morrison; 05AV-11A) | | Std | 24 | 7.9 | 0.56 | 0.54 | 57 | 0.022 | 87 | 0.025 | 85 | 2.5 | 94 | 10 | |
| ***Pyrrhotite*** | | | | | | | | | | | | | | | |
| Contact | 8 | Ave | 0.38 | 4.34 | 1.57 | bdl | 154 | 0.093 | 1.87 | 0.085 | 37.9 | bdl | bdl | 2.15 | bdl |
| (Levack; 99AV-122) | | Std | 0.14 | 0.40 | 0.26 | | 45 | 0.056 | 0.59 | 0.016 | 2.2 | | | 0.93 | |
| Transition | 7 | Ave | 0.333 | 2.86 | 0.241 | bdl | 22.5 | 0.45 | 2.09 | 0.055 | 81.8 | 0.10 | bdl | 1.80 | bdl |
| (Morrison; 08AV-08) | | Std | 0.063 | 0.17 | 0.079 | | 2.5 | 0.67 | 0.71 | 0.013 | 3.9 | 0.13 | | 0.78 | |

Note: bdl = below detection limit; n = sample size

**Figure 3.** Examples of trace elements in major sulphides that can be used to discriminate between different ore types. **a)** Cd vs. Se content in chalcopyrite. **b)** As vs. Se content in pentlandite. **c)** Co vs. Se content in pentlandite. **d)** Co vs. Se content in pyrrhotite. Data for McCreedy East samples are from Dare et al. (2011).

Partition coefficients of trace elements in chalcopyrite, pentlandite, and pyrrhotite were calculated for contact, transitional, and sharp-walled veins. Partition coefficients are affected by intensive variables, such as temperature, pressure, oxygen fugacity, sulphur fugacity, etc. (e.g. Mungall et al, 2005). All these variables are indicators of the mineralization environment; hence, differences in partition coefficients are reliable indicators of different processes of formation. The propagated uncertainties for most of the elements that were analysed are too large for meaningful comparisons; however, the partition coefficient ($\pm$ 2$\sigma$) of Se between chalcopyrite and pentlandite is 1.2 $\pm$ 0.1 for contact and transition ores but only 0.5 $\pm$ 0.2 for vein-

type ores, indicating that veins formed by different process than contact and transition ores (e.g. Hanley et al., 2005; Pentek et al., 2013).

## Element Distribution Maps of Sulphide Assemblages

Zonation of trace elements, including some HSE, in pyrite from contact ore (Levack) was documented; no HSE was detected in the major sulphides (pyrrhotite, chalcopyrite, pentlandite). Figure 4 illustrates some of the most significant features that were observed. The area mapped contains a trapezoidal section of one euhedral pyrite grain surrounded by pyrrhotite, chalcopyrite, and minor pentlandite (Fig. 4a). Some small
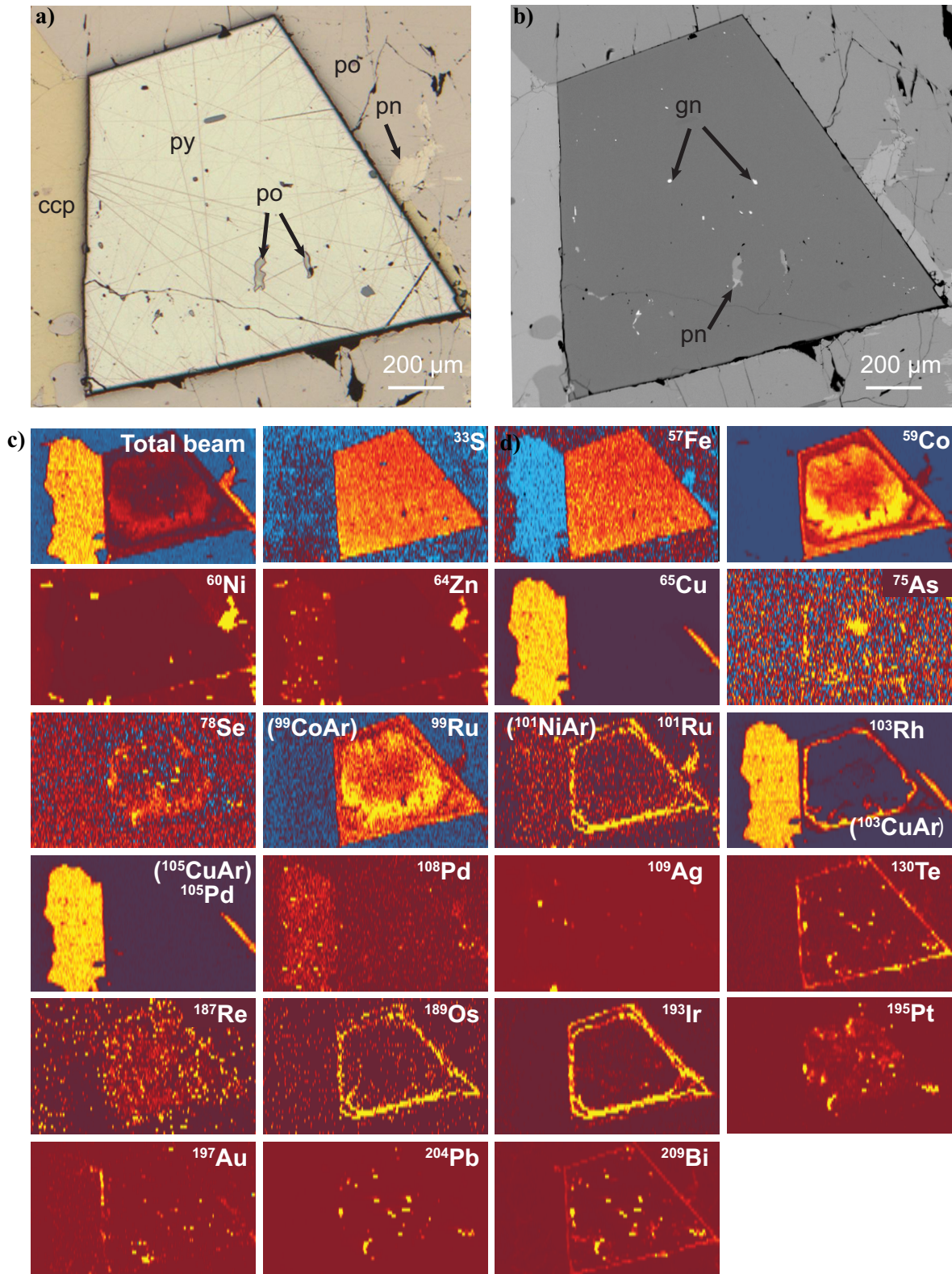
**Figure 4.** LA-ICP-MS trace element mapping of euhedral pyrite (py) and surrounding pyrrhotite-pentlandite-chalcopyrite (po-pn-ccp) assemblage from contact ore, Levack deposit. **a)** Reflected light photomicrograph for reference. **b)** Backscattered electron image of the same slide as (a) showing inclusions of galena (gn) and other sulphides (e.g. pentlandite) in pyrite. **c)** Element distribution maps (in relative signal intensities) of the same slide. No significant trace element concentrations were detected in the major sulphides. However, pyrite displays (i) a complex zoning of Co, Se, and As; (ii) thin rims containing Ru, Rh, Os, Ir, Te, and Bi, as well as discrete inclusions containing Pt, Au, Pb, Bi, and Te. Maps use a 'warm-cold' scale with yellow being of highest relative intensity, and blue lowest). The signal shown is not corrected for argide-metal interferences of lighter isotopes on higher masses (e.g. $^{59}Co$, $^{63}Cu$, $^{65}Cu$ on $^{99}Ru$, $^{103}Rh$, $^{105}Pd$, respectively) or isobaric interferences (e.g. $^{108}Cd$ on $^{108}Pd$).
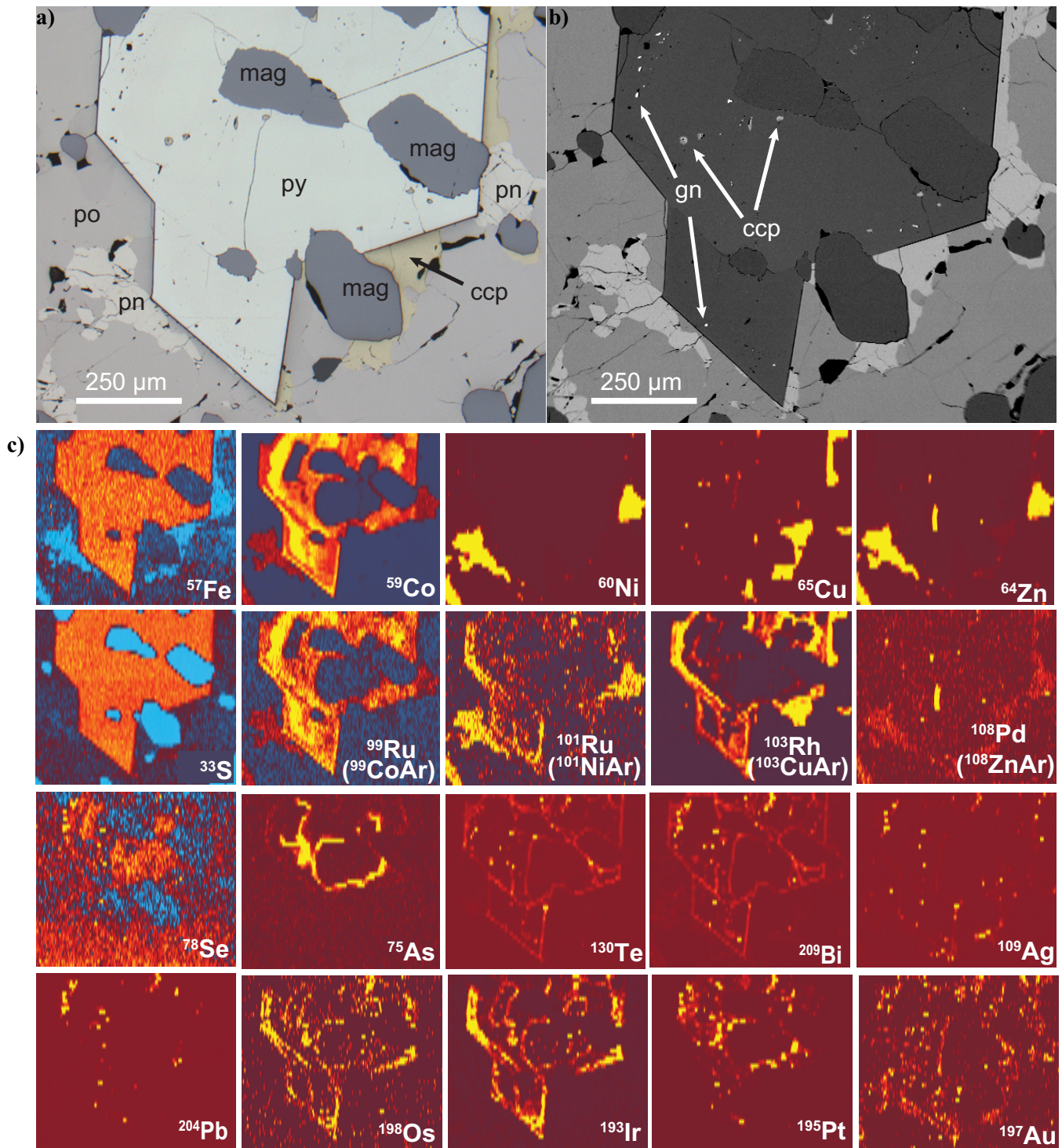
**Figure 5.** LA-ICP-MS trace element mapping of a composite pyrite (py) grain from contact ore, Levack deposit. **a)** Reflected light photomicrograph showing a large euhedral composite grain of pyrite, enclosing anhedral magnetite (mag) and surrounded by chalcopyrite (ccp), pentlandite (pn), and pyrrhotite (po). **b)** BEI highlighting small galena (gn) and chalcopyrite inclusions in the pyrite grain. **c)** Element distribution maps showing complex zoning of Se, As, and Co (e.g. areas with relatively high Se have no detectable Co; high As areas 'outline' Se-rich areas and are then surrounded by complex Co zonation). The distribution of Ru, Rh, Os, and Ir matches regions within the Co-rich zoned pyrite that are close to the edges of the grain. The Te and Bi distribution outline pyrite grain boundaries and subdomains. The distribution of Pt in pyrite matches that of As and also some discrete Bi as well as some of the galena inclusions.

galena inclusions were observed within pyrite but no HSE-bearing minerals were detected (Fig. 4b). Figure 4c is a set of element distribution maps on a yellow-blue (warm-cold) colour scale. Each map is normalized to the highest signal intensity for the element represented; thus the maps are not meant to provide information (or comparisons) about element concentrations but to illustrate element zonation and rims (e.g. Co, Ru, Rh, Os, Ir, Te, and Bi in pyrite) as well as the presence and distribution of micrometre- and nanometre-scale nuggets (e.g. Te, Pt, Au, Pb, and Bi in pyrite). Figure 5 shows a more complex element zonation of pyrite and again illustrates that most trace elements of interest are dominantly in pyrite rather than chalcopyrite, pentlandite, or pyrrhotite. The maps (Fig. 5c) illustrate several stages of growth in pyrite: (i) a Co-poor but relatively Se-rich stage (centre of the composite grain), followed by (ii) an As-rich stage, followed by (iii) growth of Co-rich areas. Four HSE elements (Ru, Rh, Os, and Ir) are present mostly near the euhedral grain edges of the composite pyrite grain. Tellurium and Bi seem to delineate fractures and the boundaries of the subgrains within the pyrite grains. What is most significant about Co-rich, HSE-bearing pyrite is that it records the geochemical processes that affected the distribution of HSE and key elements (As, Bi, Te). These elements were involved in the formation of the most common platinum group metals in the footwall ores (e.g. merenskyite, moncheite, sperrylite; Cabri and LaFlamme, 1976). Thus, understanding the origin of such pyrite should provide valuable information about the ore-forming processes.

## IMPLICATIONS FOR EXPLORATION

These results provide several insights that are relevant for exploration in the challenging footwall environment. Fingerprinting of distinctive trace element signatures can help identify each of the mineralization types present (i.e. contact, transition, sharp-walled veins, disseminated) which further can aid in identify the processes of their formation. The Se content in major sulphides was shown to increase with depth and when compared with Se content in slightly altered contact-style samples from McCreedy East (Fig. 3), indicates that this increase is likely due to hydrothermal activity. Partition coefficients for Se in chalcopyrite and in pentlandite are similar for contact and transition ores but are different for Se in chalcopyrite and in pentlandite from sharp-walled veins, indicating that contact and transition ores may share the same origin but that sharp-walled veins were produced under different conditions. This supports the concept that the contact and transition ores were formed through magmatic processes but that different processes, likely a magmatic-hydrothermal origin have affected the sharp-walled veins. No PGEs were detected in any of the major sulphide minerals (pyrrhotite, pentlandite, chalcopyrite) but pyrite from contact ore displayed complex zoning of many trace elements, including Co, Se, As, and several PGE elements, notably Ir and Os. Although the origin of this pyrite is not clear, it is of significance as it may provide important information about the mineralization processes. For example, if it can be shown that the Co-rich, PGE-bearing pyrite was of magmatic origin (i.e. by cooling of an immiscible sulphide melt) then the presence of pyrite with similar characteristics (even in small amounts) in footwall ores would be a marker of sulphide melt infiltration (for example, transition ore samples contain anhedral pyrite grains with relatively high As and Pt cores). Alternatively, if it can be shown that the Co-rich, PGE-bearing pyrite was of hydrothermal origin, then the presence of such pyrite in contact ores would indicate that contact ores were affected by hydrothermal processes. However, at present there is not enough data to properly constrain the origin of Co-rich, PGE-bearing pyrite.

## FORTHCOMING PRODUCTS

Two papers are in preparation for submission (spring 2015) to peer-reviewed journals. The first paper discusses the trace element content of the major sulphides in the contact and footwall of the Levack-Morrison ore system, with focus on trace elements (e.g. Se, Co, Cd) that have potential for discriminating among different ore types. The second paper documents the trace element distribution maps, the complex zoning in pyrite, and the potential implications of the presence of Co-rich, PGE-bearing pyrite for exploration.

## ACKNOWLEDGEMENTS

## REFERENCES

Ames, D.E. and Farrow, C.E.G., 2007. Metallogeny of the Sudbury mining camp, Ontario, *In:* Mineral Deposits of Canada: A Synthesis of Major Deposit Types, District Metallogeny, the Evolution of Geological Provinces, and Exploration Methods, (ed.) W.D. Goodfellow; Geological Association of Canada, Mineral Deposits Division, Special Publication No. 5, p. 329–350.

Ames, D.E. and Kjarsgaard, I.M., 2013. Sulphide and alteration mineral chemistry of low- and high-sulphide Cu-PGE-Ni deposits in the footwall environment, Sudbury, Canada; Geological Survey of Canada, Open File 7331.

Cabri, L.J. and Laflamme, J.H.G., 1976. The Mineralogy of the platinum-group elements from some copper-nickel deposits of the Sudbury area, Ontario; Economic Geology, v. 71, p. 1159–1195.

Dare, S.A.S., Barnes, S-J., Prichard, H.M., and Fisher, P.C., 2011. Chalcophile and platinum-group element (PGE) concentrations in the sulphide minerals from the McCreedy East deposit, Sudbury, Canada, and the origin of PGE in pyrite; Mineralium Deposita, v. 46, p. 381–407.

Farrow C.E.G. and Watkinson, D.H., 1997. Diversity of precious metal mineralization in footwall Cu-Ni-PGE deposits, Sudbury, Ontario: implications for hydrothermal models of formation; The Canadian Mineralogist, v. 35, p. 817–839.

Gibson, A., 2010. Contrasting styles of mineralization: North Range 148 zone versus South Range 109 FW zone, *In:* Abstracts, 11th International Platinum Symposium, 21–24 June 2010, Sudbury, Ontario, (ed.) G.H. Brown, P.L. Jugo, C.M. Lesher, and J.E. Mungall; Ontario Geological Survey, Miscellaneous Release-Data 269.

Hanley, J.J., Mungall, J.E., Pettke, T., Spooner, E.T.C., and Bray, C.J., 2005. Ore metal redistribution by hydrocarbon brine and hydrocarbon-halide melt phases, North Range footwall of the Sudbury Igneous Complex, Ontario, Canada; Mineralium Deposita, v. 40, p. 237–256.

Kjarsgaard, I.M. and Ames, D.E., 2010. Ore mineralogy of Cu-Ni-PGE deposits in the North Range footwall environment, Sudbury, Canada, *In:* Abstracts, 11th International Platinum Symposium, 21–24 June 2010, Sudbury, Ontario, (ed.) G.H. Brown, P.L. Jugo, C.M. Lesher, and J.E. Mungall; Ontario Geological Survey, Miscellaneous Release Data 269.

Morrison G.G., Jago B.C., and White T.L., 1994. Footwall mineralization of the Sudbury Igneous Complex. *In:* Proceedings of the Sudbury–Noril'sk symposium, (ed.) P.C. Lightfoot and A.J. Naldrett; Ontario Geological Survey, Special Volume 5, p. 57–64.

Mungall J.E., Andrews, D.R.A., Cabri, L.J., Sylvester, P.J., and Tubrett, M., 2005. Partitioning of Cu, Ni, Au, and platinum-group elements between monosulfide solid solution and sulfide melt under controlled oxygen and sulfur fugacities; Geochimica et Cosmochimica Acta, v. 69, p. 4349–4360.

Nelles, E.W., 2012. Genesis of Cu-PGE-rich footwall-type mineralization in the Morrison deposit, Sudbury; M.Sc. thesis, Laurentian University, Sudbury, Ontario, 96 p.

Pentek, A., Molnar, F., Tuba, G., Watkinson, D.H., and Jones, P.C., 2013. The significance of partial melting processes in hydrothermal low-sulfide Cu-Ni-PGE mineralization within the footwall of the Sudbury Igneous Complex, Ontario, Canada; Economic Geology, v. 108, p. 59–78.

Stewart, M.C. and Lightfoot, P.C., 2010. Diversity in platinum group element (PGE) mineralization at Sudbury: New discoveries and process controls, *In:* Abstracts, 11th International Platinum Symposium, 21–24 June 2010, Sudbury, Ontario, (ed.) G.H. Brown, P.L. Jugo, C.M. Lesher, and J.E. Mungall; Ontario Geological Survey, Miscellaneous Release Data 269.